Nonlin. Processes Geophys., 13, 205–222, 2006
www.nonlin-processes-geophys.net/13/205/2006/

Nonlinear Processes in Geophysics

Numerical simulation of helical-vortex effects in Rayleigh-Bénard convection

G. V. Levina and I. A. Burylov

Institute for Continuous Media Mechanics, UB RAS, Perm, Russia

Received: 16 January 2006 – Revised: 24 March 2006 – Accepted: 24 March 2006 – Published: 21 June 2006

Abstract. A numerical approach is substantiated for searching for the large-scale alpha-like instability in thermoconvective turbulence. The main idea of the search strategy is the application of a forcing function which can have a physical interpretation. The forcing simulates the influence of small-scale helical turbulence generated in a rotating fluid with internal heat sources and is applied to naturally induced fully developed convective flows. The strategy is tested using the Rayleigh-Bénard convection in an extended horizontal layer of incompressible fluid heated from below. The most important finding is an enlargement of the typical horizontal scale of the forming helical convective structures accompanied by a cells merging, an essential increase in the kinetic energy of flows and intensification of heat transfer. The results of modeling allow explaining how the helical feedback can work providing the non-zero mean helicity generation and the mutual intensification of horizontal and vertical circulation, and demonstrate how the energy of the additional helical source can be effectively converted into the energy of intensive large-scale vortex flow.

1 Introduction

Thermal convection driven by a temperature non-homogeneity is one of the most common modes of fluid and gas flow. In the atmosphere non-uniform heating results in the formation of convective circulations of different scale and frequently serves as a source of turbulence. Turbulent convective motions in rotating systems such as planet atmospheres become helical and mirror non-symmetrical (Moffatt, 1978; Parker, 1979). Small-scale helical turbulence has a number of special features and under certain conditions is capable of intensifying and sustaining large-scale vortex disturbances by means of energy transfer from small to large scales. The generating properties of small-scale helical turbulence leading to the large-scale structure formation were first discovered in magnetohydrodynamics by Steenbeck et al. (1966); Krause and Rädler (1980). This phenomenon is known as the alpha-effect. The discovery of the α-effect paved the way towards a vigorous development of MHD-dynamo theory. The formal similarity of equations describing the magnetic field in a moving electrically-conducting medium and vorticity in non-conducting fluids gave an impetus to an intensive search for analogs to this phenomenon in general hydrodynamics.

The first evidence supporting the existence of similar phenomenon for a non-conducting medium was found by Moiseev et al. who discovered the hydrodynamic alpha-effect (Hα-effect) in compressible fluid for isothermal conditions (Moiseev et al., 1983b) and incompressible convectively unstable fluid (Moiseev et al., 1988). Based on the results (Moiseev et al., 1983b) a physical mechanism was proposed for enhancing large-scale vortex disturbances in the atmosphere using the energy of small-scale helical turbulence (Moiseev et al., 1983a). In further works they extended this idea and developed a theory of the turbulent vortex dynamo in hydrodynamics of non-conducting fluid.

Frisch et al. (1987) provided not only theoretical grounds for the existence of the anisotropic kinetic alpha-effect (AKA-effect), but supported their finding by full simulations of the three-dimensional Navier-Stokes equations. This kinetic (non-MHD) large-scale instability may develop in incompressible three-dimensional anisotropic flows lacking parity-invariance. In the last decade a number of interesting studies have dealt with the application of the AKA-effect to describe the processes occurring in density-stratified differentially rotating astrophysical bodies: Kitchatinov et al. (1994), Pipin et al. (1996), and some others cited by Brandenburg and v. Rekowski (2001) who discussed the astrophysical significance of the AKA-effect.

Correspondence to: G. V. Levina
(levina@icmm.ru)

Published by Copernicus GmbH on behalf of the European Geosciences Union and the American Geophysical Union.

The early model (Moiseev et al., 1988) of the large-scale alpha-like instability generated by the interaction between the convective flow in an extended horizontal layer heated from below and prescribed external small-scale helical turbulence of non-convective origin was generalized by Rutkevich (1993) to a natural case of convective turbulence in a rotating layer heated from below and by internal heat sources. This was a demonstration that the concept of helical turbulence suggests a parameterization of the combined effect of the Coriolis force and the additional to the heating from below energy flux generated, for example, by internal heat release due to vapor condensation.

In the field of atmospheric research Kurgansky reached the same conclusion independently (Kurgansky, 1993, 1998, 1999). These investigations are summarized in Sect. 4.1 of Kurgansky's recent book (Kurgansky, 2002). This was probably one of the very first attempts to introduce the most extensive theories regarding helicity into meteorological monographs and giving the most general helicity balance equation in a rotating compressible fluid. Kurgansky showed that under moist convection in a rotating fluid an additional energy release due to phase transition of moisture is just the condition required to achieve the non-zero dynamo-effect and developed a theoretical model for the turbulent vortex dynamo (Kurgansky, 1998, 1999). Kurgansky's model contained the helicity balance equation for the small-scale turbulent velocity field in addition to a linear equation for the mean vorticity generation on large scales similar to the $H\alpha$-effect equation in Moiseev et al. (1988). This allowed the restriction of the growth of large-scale instability and achieved saturated i.e. stationary states what could be considered as further progress towards a more realistic dynamo model.

Thus, a number of factors have been defined which are found to be necessary for the existence of the hydrodynamic α-effect in conditions of non-uniformly heated medium: thermoconvective turbulence, rotation, internal heat sources. In the authors' opinion, it is worthy of note that the energy release in water phase transitions may not be the only internal source of heat. In nature, the formation of helical atmospheric vortices can be sustained by the additional energy of both heat release due to condensation of vapor (cloud vortices-tornadoes, waterspouts and tropical cyclones) and intensely heated solid particles in conditions of dry convection (dust devils). We expect that the Hα-effect in thermoconvective turbulence may result in a large-scale hydrodynamic (non-MHD) instability of a new type that may really exist in Nature, namely, helical-vortex instability (Levina et al., 2000).

To support the theoretical hypothesis on generating properties of small-scale helical turbulence a series of laboratory experiments started at the Institute of Continuous Media Mechanics and Perm State University in the late 1980s. Some of them resulted in promising findings surveyed in Levina et al. (2000), amongst which a laboratory large-scale intensive spiral vortex generated from a localized heat source in a rotating turbulent fluid is of particular interest (Bogatyryov, 1990; Bogatyryov and Smorodin, 1996). When interpreting the discovered effect an idea was advanced that the small-scale helicity of the rising thermals from the temperature boundary layer might be responsible for the onset of crisis situation favoring the development of large-scale disturbance with a structure of helical vortex. A thorough investigation of the velocity field of this laboratory vortex (Bogatyryov and Smorodin, 1996) revealed a similarity to the velocity field of tropical cyclones. These experiments were restarted at our laboratory recently (Kolesnichenko et al., 2002; Bogatyryov et al., 2006). They are focused on the modeling of physical mechanisms and conditions leading to the formation of intensive atmospheric vortices and aimed at obtaining the quantitative results by means of modern Particle Image Velocimetry technique. This is giving us an additional impetus to develop the appropriate numerical approach for comprehensive studying the helical-vortex phenomena in thermoconvective turbulence.

The paper is organized as follows. In Sect. 2 a way to simulate the large-scale helical-vortex instability in a convectively unstable fluid is proposed, a forcing function to introduce into the Boussinesq equations is derived and resulting balance equations for energy and helicity are examined. In Sect. 3 the governing equations are given, in Sect. 4 they are adapted for numerical modeling, and the numerical realization is discussed. The numerical results are described in details in Sect. 5. Section 6 offers our two-stages strategy for numerical simulation of the helical-vortex instability and conclusions concerning the results obtained at the first stage. Two appendices are included: (A) to describe the mean-field equation with the alpha-term generating the vortex dynamo effect and (B) to discuss the results of the linear stability analysis.

2 Helical-vortex convection: problem formulation and conservation laws

The first mean-field equation of the Hα-effect in a convective system was obtained by the statistical averaging method (Moiseev et al., 1988). It described the influence of small-scale helical turbulence on the classical Rayleigh-Bénard convection in a plane infinite horizontal layer of incompressible liquid heated from below.

The most demonstrative physical interpretation of the obtained effect can be given in terms of toroidal and poloidal component of the vectorial velocity field (Moffatt, 1978), i.e. in the form of representation that is frequently used in magnetohydrodynamics and is well suited for transformation of corresponding vector equations to the system of equations for scalar functions. Let us choose $\boldsymbol{V}$ for denoting the mean velocity field $\langle v_i \rangle$ and express it in the following form:

$$\boldsymbol{V} = \boldsymbol{V}_T + \boldsymbol{V}_P \,, \; \boldsymbol{V}_T = \mathrm{curl}\,(\boldsymbol{e}\,\psi) \,, \; \boldsymbol{V}_P = \mathrm{curl}\,\mathrm{curl}\,(\boldsymbol{e}\,\phi) \,.$$

Now a mathematical model of helical-vortex convection in the simplest representation allowing for the new large-scale instability can be written as (Levina et al., 2000, 2001, 2004):

$$\left(Pr\frac{\partial}{\partial t}-\Delta\right)T=-\Delta_{\perp}\phi\,,$$
$$\left(\frac{\partial}{\partial t}-\Delta\right)\Delta\phi=Ra\,T+S\left[(\boldsymbol{e}\,\nabla)^2-\Delta_{\perp}\right]\psi\,, \qquad (1)$$
$$\left(\frac{\partial}{\partial t}-\Delta\right)\psi=-S(\boldsymbol{e}\,\nabla)^2\phi\,,$$

$$Pr=\frac{\nu}{\chi}\,,\quad Ra=\frac{g\beta Ah^4}{\nu\chi}\,,\quad \boldsymbol{e}=\{0,0,1\}\,.$$

Here, T is the temperature, ψ and ϕ are the toroidal and poloidal potentials of the velocity field, and $\Delta_{\perp}=\partial^2/\partial x^2+\partial^2/\partial y^2$ is the two-dimensional Laplace operator. Pr and Ra are the Prandtl and Rayleigh numbers, $\boldsymbol{e}$ the unit vector directed vertically upward, A the uniform temperature gradient between the horizontal boundaries of the layer, g the gravity acceleration, β the coefficient of thermal expansion, h the layer height. The dimensionless parameter S characterizing the small-scale turbulence is related in a rather complicated manner to the coefficients of kinematic viscosity ν and thermal diffusivity χ, the turbulence characteristics such as the most energetic scale λ and characteristic time τ of the turbulent velocity correlation. Of fundamental importance is its proportionality to the mean value of the scalar product of the turbulent velocity $\boldsymbol{v}^T$ by the vorticity – $S\sim\langle\boldsymbol{v}^T\cdot\mathrm{curl}\,\boldsymbol{v}^T\rangle$, what owes its origin to the assumption of the prescribed helicity of turbulence. The explicit representation of the parameter S is given in Moiseev et al. (1988).

The system of dynamic linear equations (Eq. 1) for three large-scale fields includes two different positive feedbacks. One of them acts between the poloidal ϕ-component of the velocity field and the field of temperature disturbance T. It links the first and the second equations in system (1) and leads to natural convective instability. The other directly links the solenoidal components ϕ and ψ of the velocity field, i.e. the second and the third equations from system (1). This feedback, being related to specific properties of small-scale helical turbulence, is sustained only through the parameter S. Therefore, let us name it the helical feedback. If $S\neq0$, then flow $\boldsymbol{V}$ shows a new topological property – the linkage of the vortex lines of toroidal and poloidal flow component. The positive helical feedback would be expected to cause a new type of instability.

Within the model (1), the large-scale instability in the layer with free boundaries was discovered in the same work (Moiseev et al., 1988) whilst for other types of boundary conditions it was found slightly later (Lyubimov and Smorodin, 1989; Berezin and Zhukov, 1990). Those investigations were carried out within the framework of the linear and nonlinear theory of hydrodynamic stability. They have demonstrated that the intensification of the helical feedback (an increase of the helicity parameter S) causes a decrease in the threshold of convective instability and enlargement of the characteristic horizontal scale of arising convective motions. As soon as the helicity parameter reaches critical value, S^{cr}, the wave number vanishes. Formally, this corresponds to an infinite horizontal dimension of a supercritical flow and suggests qualitative changes in the flow pattern: the system of small cells with a characteristic horizontal scale of order of layer height, normally observed as Rayleigh-Bénard convection, should be rearranged into a single large vortex, which tends to occupy the entire available space. According to Eq. (1), the toroidal and poloidal components of the large-scale velocity field in such vortices should be linked, forming thereby a helical structure of large-scale circulation.

Thus, it has been demonstrated that the action of small-scale helical turbulence within the Rayleigh-Bénard convection may initiate a new large-scale instability – the helical-vortex.

The analysis of investigations on helical-vortex instability in a convective system carried out in review by Levina et al. (2000) has revealed a number of crucial points which are specified below.

All currently available mean-field models of Hα-effect in a convectively unstable fluid are found to include linear evolution equations for the large-scale velocity field and have exponentially growing solutions. At this stage no one presenting this way of theoretical research (Moiseev et al., 1988; Rutkevich, 1993; Levina et al., 2000) has obtained any nonlinear terms for the mean-field velocity equation capable of restricting the instability growth within these models. This makes them inapplicable to simulate any steady mean flow by numerical calculations.

On the other hand, review (Levina et al., 2000) outlined a clear sign indicating the onset of helical-vortex instability: the initiation of positive helical feedback between the toroidal and poloidal components of the vector velocity field. Such feedback may be generated in a helical eddy cell in which the velocity field is characterized by a linkage of the vortex lines of toroidal and poloidal flow components, i.e. by non-zero helicity $\boldsymbol{v}\cdot\mathrm{curl}\,\boldsymbol{v}\neq0$.

It has served as a basic idea for developing a numerical approach by Levina et al. (2001, 2004) to study the evolution of helical-vortex instability in conditions of turbulent thermal convection. A key to the approach is the addition of a model force to the convection equations.

It is widespread in turbulence modeling to have a forcing function driving a turbulent flow. However, the forcing term in our simulation is not assigned to be a driving force. It is applied to naturally induced, fully developed convective flows and is assumed to be responsible for the generation of a helical flow structure with $\boldsymbol{v}\cdot\mathrm{curl}\,\boldsymbol{v}\neq0$ and positive helical feedback. Probably, the best forcing for this purpose is the

generating α-term from the mean-field velocity equation describing the Hα-effect in a convective system (Moiseev et al., 1988; Rutkevich, 1993; Levina et al., 2000).

2.1 Forcing term to generate the positive helical feedback

Numerical simulation based on the nonlinear Boussinesq equations has been suggested. Within this approach the momentum equation is additionally supplied with a model force. The computational algorithm will be discussed in detail in the corresponding section of this work.

The model force is assumed to be a variable whose tensor structure is identical to that of the generating alpha-term (the corresponding mean-field Eq. (A2) is given and discussed in Appendix A). Indeed, in physical terms the alpha-term represents a force, whose explicit form can be obtained by a few manipulations on the right of expression (A2):

$$\boldsymbol{f} = s_1\{\boldsymbol{e}\,(\mathrm{curl}\,\boldsymbol{V})_z - \partial(\boldsymbol{e}\times\boldsymbol{V})/\partial z\}\,, \tag{2}$$

where $\boldsymbol{V}$ is the vector notation for the mean velocity field $\langle v_i\rangle$, $\boldsymbol{e}$ is the unit vector along the vertical axis z.

In Moiseev et al. (1988); Rutkevich (1993), the mean field equation was derived whilst being subject to a great number of simplifying and limiting assumptions resulting in the variety of physical and geometrical parameters entering the coefficient s_1. In order to avoid an over complication we may deduce that the variable $\boldsymbol{f}$ in our numerical approach is a model force. Bearing in mind that the basic intent of model force is to generate helical structure of the flow with positive helical feedback, it seems to be natural to interpret this coefficient as an intensity of the initiated feedback. Deriving the explicit form of this coefficient is based on the following.

Indeed, the correct introduction of a new term in an equation suggests the conservation of symmetry and dimension properties of the initial equation.

All terms entering the momentum equation from the Boussinesq system are the polar vectors (Chandrasekhar, 1961; Gershuni and Zhukhovitsky, 1972) whereas both terms in expression (2) are pseudo vectors. Therefore, to conserve the symmetry, one should introduce a pseudo scalar variable into the coefficient in front of the model forcing function. Physical formulation of the problem and the results of Rutkevich (1993) indicate that the angular velocity of liquid rotation Ω is an adequate variable. In correspondence with the dimension requirement this quantity should be multiplied by characteristic length which is assumed to be the layer height h. An additional point to be remembered is that to describe the geophysical flow in a rotating layer one usually takes the Coriolis parameter which is equal to twice the angular velocity 2Ω.

Now the model forcing function may be written in dimensional form as

$$\boldsymbol{f} = 2\Omega h\,\{\boldsymbol{e}\,(\mathrm{curl}\,\boldsymbol{V})_z - \partial(\boldsymbol{e}\times\boldsymbol{V})/\partial z\}\,. \tag{3}$$

The model force is similar to the Coriolis force in that they are both the functions of velocity, i.e. dependent on the flow to which they are applied. It might be helpful to present here the expressions describing the components of the model force $\boldsymbol{f}$ and the Coriolis force $\boldsymbol{f}^{\mathrm{Cor}}$ along the corresponding directions (x, y, z) in order to demonstrate the difference between these functions

$$\boldsymbol{f} = 2\Omega h\left\{\frac{\partial v}{\partial z},\ -\frac{\partial u}{\partial z},\ \frac{\partial v}{\partial x} - \frac{\partial u}{\partial y}\right\}; \tag{4}$$

$$\boldsymbol{f}^{\mathrm{Cor}} = 2\Omega\,\{v,\ -u,\ 0\},$$

where the velocity vector $\boldsymbol{V}$ has three components u, v, w along the directions (x, y, z), respectively.

An essential feature of the model force $\boldsymbol{f}$ is its dependence not simply on velocity but on its spatial derivatives. The latter implies that the model force, unlike the Coriolis force, works and can pump an additional energy into the system under examination. It is also evident that the z-component absent in the Coriolis force is the necessary element to close the feedback loop between the components of the velocity field. The way in which the forcing function $\boldsymbol{f}$ is involved in generation of positive feedback between the poloidal and toroidal velocity field will be explained in detail and illustrated by numerical results.

2.2 Energy and helicity balance in helical-vortex convection

It seems useful to write down the energy and helicity balance equations in these new conditions in view of the helical feedback will pump an additional energy into the system and should also generate the non-zero mean helicity.

Following the similar way as in Golitsyn (1979); Busse (1981); Frisch (1995) the appropriate balance equations for convection in a horizontal layer of incompressible fluid based on the Boussinesq approximation can be obtained in the following form:

$$\begin{aligned}
&\frac{d}{dt}\left\langle\frac{\boldsymbol{V}\cdot\boldsymbol{V}}{2}\right\rangle = g\beta\,\langle w\,T\rangle - \nu\left\langle|\boldsymbol{\omega}|^2\right\rangle + \\
&\qquad + 2\Omega h\left(\langle w\,\omega_z\rangle + \left\langle(\boldsymbol{e}\times\boldsymbol{V})\cdot\frac{\partial\boldsymbol{V}}{\partial z}\right\rangle\right),\\
&\frac{d}{dt}\left\langle\frac{T\cdot T}{2}\right\rangle = \langle w\,T\rangle - \chi\left\langle|\nabla T|^2\right\rangle, \qquad (5)\\
&\frac{d}{dt}\left\langle\frac{\boldsymbol{V}\cdot\boldsymbol{\omega}}{2}\right\rangle = g\beta\,\langle\omega_z\,T\rangle - \nu\,\langle\boldsymbol{\omega}\cdot\mathrm{curl}\,\boldsymbol{\omega}\rangle + \\
&\qquad + 2\Omega h\left(\langle\omega_z^2\rangle - \left\langle\left(\frac{\partial\boldsymbol{V}}{\partial z}\right)^2\right\rangle\right),
\end{aligned}$$

$$\boldsymbol{\omega} = \mathrm{curl}\,\boldsymbol{V}\,, \qquad \boldsymbol{V} = \{u, v, w\}\,, \qquad \boldsymbol{\omega} = \{\omega_x, \omega_y, \omega_z\}\,,$$

where: $\boldsymbol{\omega}$ is the vorticity and angular brackets denote spatial averaging.

For stationary flows the expressions on the left of balance equations are equal to zero. Thus, for stationary free convection without any forcing the energy balance is described by the first two terms on the right of the velocity and temperature equations (Golitsyn, 1979; Busse, 1981): this implies a balance of buoyancy and viscosity forces in the first case and a balance of convective heat transfer and entropy production in thermal convection in the second equation. No helicity generation takes place in free convection without rotating effects.

As it follows from the above equations, model forcing function (3) does operate contributing to both the energy and helicity balances. However, in both cases we cannot make any definite estimations based only on balance equation analysis. A contribution to the energy balance is described as a sum of two alternating-sign terms, and to the helicity balance the forcing function contributes two terms of constant but different signs. Although the forcing does not contribute explicitly to the temperature equation, yet it should influence the convective heat transfer via affecting the velocity field. Therefore, a numerical analysis seems to be the most effective way to clear up this question. In fact, we will give some estimations for different terms in balance equations (Eq. 5) in due course.

3 The governing equations

We investigate helical convective flows initiated in an extended horizontal layer of incompressible fluid which is bounded above and below by surfaces sustained at constant and different temperatures.

A mathematical model involves the nonlinear Boussinesq equations, in which the momentum equation in addition includes forcing function (3) (Levina et al., 2001, 2004):

$$\begin{gathered}\frac{\partial \boldsymbol{V}}{\partial t}+\frac{1}{Pr}\boldsymbol{V}\nabla\boldsymbol{V}=-\nabla p+\triangle\boldsymbol{V}+RaT\boldsymbol{e}+Re^{\Omega}\boldsymbol{f},\\ Pr\frac{\partial T}{\partial t}+\boldsymbol{V}\nabla T=\triangle T,\quad \mathrm{div}\boldsymbol{V}=0,\\ \boldsymbol{f}=\boldsymbol{e}\cdot(\mathrm{curl}\,\boldsymbol{V})_z-\frac{\partial(\boldsymbol{e}\times\boldsymbol{V})}{\partial z},\quad \boldsymbol{e}=\{0,0,1\},\\ Ra=\frac{g\beta(T_1-T_2)h^3}{\nu\chi},\quad Pr=\frac{\nu}{\chi},\quad Re^{\Omega}=\frac{2\Omega h^2}{\nu}.\end{gathered}\tag{6}$$

Here: p is the pressure, (T_1-T_2) the typical temperature difference between horizontal boundaries of the layer, We have chosen the layer height h, the typical temperature difference (T_1-T_2), the combinations h^2/ν, χ/h and $\rho_0\nu\chi/h^2$ as the units to measure length, temperature, time, velocity and pressure, respectively.

The dimensionless criterion in front of the model forcing function $\boldsymbol{f}$ is found to be exactly equal to that before the Coriolis force in the momentum equation describing convection in rotating fluid, i.e. the Taylor number – $Ta^{1/2}$. However, allowing for the difference between two above mentioned forces (Eq. 4) in order to avoid any tanglement, we denote this number Re^{Ω} – the Reynolds number defined by a characteristic value of the angular velocity Ω. This new dimensionless parameter characterizes the intensity of the helical feedback between the toroidal and poloidal component of the velocity field.

Equations (6) describe a mixed convection flow at $Ra\neq0$ and $Re^{\Omega}\neq0$. The special case $Re^{\Omega}=0$ corresponds to that the helical feedback is absent, and system (6) is reduced to the Boussinesq equations describing free convection. Another possibility is connected with vortex flows driven by the helical forcing at $Re^{\Omega}\neq0$ in an isothermal situation at $T=$const and consequently, $Ra=0$.

New theoretical model (Eq. 6) was first analyzed in terms of the linear theory of hydrodynamic stability (see Appendix B).

The linear stability analysis showed that the positive helical feedback introduced into the convective system can initiate a long wave instability appearing at much lower Rayleigh numbers than the natural convective instability. The analysis also resulted in preliminary estimations for the range of parameter variations to use in numerical calculations.

4 Numerical implementation

The proposed approach for searching for the large-scale alpha-like instability is first applied to the 3-D laminar Rayleigh-Bénard convection in an incompressible fluid layer extended in horizontal directions and heated from below. A remarkable feature of the Rayleigh-Bénard problem is that its solution for a laminar state represents a great number of similar convective cells. In our approach they can be considered as structures of an intermediate scale. The forcing term making the flow helical and pumping the energy into the system simulates the influence of small-scale helical turbulence. Thus, a contribution of different scale flows is taken into consideration. Further, in the context of the global alpha-effect hypothesis, an intriguing question arises: is it possible to simulate some signs of large-scale helical-vortex instability whilst operating in these relatively simple conditions?

Initially, we are trying to discover the phenomena related to an excitation of the helical-vortex instability by using the most accessible computational techniques with a minimum expenditure of time. The simplest mathematical formulation of the problem involving helical-vortex effects is obtained for the flow in the cylindrical geometry domain with axial symmetry. In this case, all three components of the velocity vector are retained ensuring the non-zero helicity $\boldsymbol{V}\cdot\mathrm{curl}\boldsymbol{V}\neq0$, whereas all physical fields become dependent on only two spatial variables.

Bearing in mind the predictions of the linear stability analysis, we allow for the possibility of the existence of supercritical motions with the horizontal scale much greater than the vertical. We choose for our simulation a bounded flow domain extended in horizontal directions, with an aspect ratio of 10.

The numerical experiment was carried out using the following scheme.

At our first stage the convective instability for low supercritical Rayleigh numbers and Re^{Ω}=0 was initiated by specifying a point vortex disturbance in the center of the computation domain at the initial time. The characteristic horizontal scale of the resulting supercritical mode and, respectively, the structure numbers in the layer (if we are dealing with the bounded region as it is in our case) are determined by a combination of the prescribed values of the parameters Pr, Ra and Re^{Ω}.

At the second stage when convective instability evolution resulted in a developed steady-state convective flow, the helical feedback was excited on this background by setting $Re^{\Omega}\neq 0$.

In this way we expect to observe a drastic rearrangement in the flow structure and discover how a broadening of convective cells may be realized. Flow evolution of this kind may simulate a similar process in turbulent flows.

4.1 Problem formulation for a cylindrical domain

Numerical realization is described in detail in Levina et al. (2004) which includes a mathematical statement of the problem in a closed form with initial and boundary conditions. We introduce the cylindrical coordinates $\{\rho, \varphi, z\}$ and consider only axially symmetrical flows ($\partial/\partial\varphi$=0). Thus, whilst maintaining the equation for azimuthal velocity v in model (6), the pressure can be eliminated from the equations by introducing the stream function Ψ and the φ-component of vorticity ω_{φ}:

$$u = -\frac{\partial \Psi}{\partial z}\,, \quad w = \frac{1}{r}\frac{\partial}{\partial r}(r\Psi)\,, \quad \omega_{\varphi} = \frac{\partial u}{\partial z} - \frac{\partial w}{\partial r}, \qquad (7)$$

where u and w are the radial and vertical velocity components.

After the above transformation, mathematical model (6) written in terms of stream function, vorticity, azimuthal velocity and temperature is found to be included three evolutionary equations and the Poisson equation for the stream function. In the set of three velocity-related variables chosen for calculation, v describes the toroidal field (horizontal circulation) whilst Ψ and ω_{φ} characterize the poloidal field (vertical circulation).

All the bounding surfaces of the cylinder were assumed to be impermeable, rigid, and non-slip. Thermal conditions included fixed temperatures at the lower and upper surfaces corresponding to the heating from below, whereas the lateral surface was adiabatic.

The numerical investigation was carried out by the method of finite differences using an explicit scheme. The Poisson equation for the stream function was solved by the successive over-relaxation method. When searching for steady flows we used a pseudo-unsteady method to solve the evolution problem in order to obtain the steady solution as $t\to\infty$.

The flow domain was assumed to have the aspect ratio of the cylinder radius to the height $R : h$ for all calculation results equal to 10:1. Thus, under the constraint of axial symmetry $\partial/\partial\varphi$=0, the computational domain represented the $R\times h$=10×1 rectangle.

In methodical calculations the discretization of computational domain varied broadly, while for obtaining basic results we used the grid 200×60 along the radius and height respectively.

4.2 Integral characteristics

To represent the results manifesting the helical-vortex instability evolution a set of characteristics have been noted which best illustrate the distinguishing features of this phenomenon.

We can anticipate that for $Re^{\Omega}\neq 0$ the helical forcing $\boldsymbol{f}$ is to make the flow helical. The forcing should also provide the positive feedback between the toroidal and poloidal component of velocity and pump some kinetic energy into the convective system in addition to the thermal energy ensured by the heating from below. That is why the following integral characteristics were introduced and analyzed:

$$S_Q = \int_Q \boldsymbol{V}\cdot\mathrm{curl}\boldsymbol{V}\,dQ\,, \qquad E_k = \frac{1}{2}\int_Q V^2\,dQ\,,$$
$$E_k^T = \frac{1}{2}\int_Q v^2\,dQ\,, \qquad E_k^P = \frac{1}{2}\int_Q (u^2+w^2)\,dQ\,. \qquad (8)$$

The velocity field characteristic S_Q can be called the total flow helicity integrated over the examined computational domain. This value specifies the motion with linked vortex lines of horizontal and vertical circulation, and its sign depends on the circulation direction in the forming vortex structures. We were also examining attentively the evolution of three other velocity-related quantities characterizing the flow energetics: the total kinetic energy E_k and separately the kinetic energy of the toroidal E_k^T (horizontal circulation) and poloidal E_k^P (vertical circulation) velocity fields.

As a quantitative measure of convective heat transfer through the layer one usually takes the Nusselt number Nu. This is the ratio of the dimensional heat transfer through the fluid layer Λ to the heat flux $\kappa(T_1-T_2)$ that can only be produced (at the same temperature difference) due to the molecular heat conductivity (Gershuni and Zhukhovitsky, 1972;

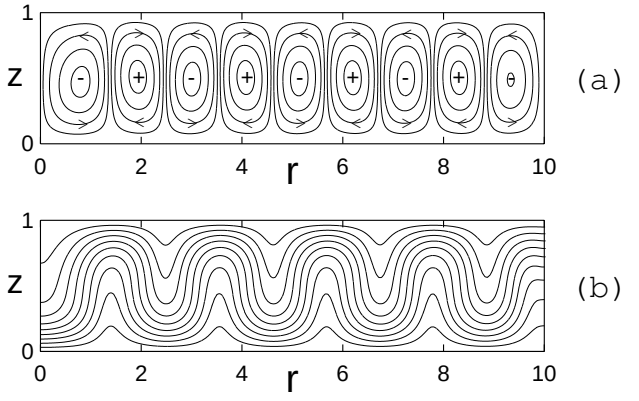

Fig. 1. Isoline maps for the stationary free convection flow at Re^{Ω}=0, Pr=1 and Ra=3000: **(a)** stream function, **(b)** temperature; r=0 corresponds to the axis of symmetry location.

Golitsyn, 1979; Busse, 1981) so that:

$$Nu = \frac{\Lambda}{\kappa(T_1 - T_2)}, \qquad \Lambda = \kappa \int_{\Gamma} \frac{\partial T}{\partial n} d\ell \,. \tag{9}$$

In these formulae $\partial T/\partial n$ is the normal component of the temperature gradient, and the integration is performed over the upper boundary Γ. Being a characteristic of the intensity of convective heat transfer the Nusselt number also allows the estimation of the intensity of convective motion.

The maximum and minimum values of all physical variables over all internal nodes of the computational domain were also found and analyzed.

In numerical experiments the Prandtl number was assumed equal to Pr=1 throughout the calculations, the Rayleigh number and the Reynolds number varied widely.

5 Basic steady-state free convective flow

Let us begin with discussing the steady-state natural convective flow to which we apply the helical forcing.

For the problem under consideration computations were carried out to define the threshold of natural convection at Re^{Ω}=0 in the horizontally extended (with aspect ratio of 10) yet bounded layer of the cylindrical geometry. They yielded the critical Rayleigh number $Ra^{\rm cr}\approx$1724. It proves to be rather close to the critical Rayleigh number for a plane infinite horizontal layer with rigid boundaries, $Ra^{\rm cr}\approx$1708, given by the linear stability theory (Gershuni and Zhukhovitsky, 1972). This is a good reason to believe that numerical simulation of helical convection ($Re^{\Omega}\neq$0) in the extended cylindrical layer may also rely on the linear analysis estimations for a plane infinite horizontal layer discussed in Appendix B.

In cylindrical geometry using the axial symmetry condition the stationary convective motions are realized as axially symmetrical annular rolls. Figure 1 presents, for example, isoline maps for a fully steady-state free convective flow at Re^{Ω}=0, Pr=1 and Ra=3000.

Table 1. Integral characteristic values for the stationary free convection flow at Re^{Ω}=0, Pr=1 and Ra=3000.

E_k	E_k^T	E_k^P	S_Ω	Nu	U_m	V_m	W_m
245	0	245	0	1.586	11.3	0.0	11.1

In the projection onto the calculation domain within the plane (r,z), the convective rolls look like the system of cells with vertical circulation. Such typical free convection circulation is created only by the poloidal velocity field which is described in our numerical approach by two scalar functions – the stream function, Ψ, and φ-component of vorticity, ω_φ, introduced by Eqs. (7). Resulting structures in the velocity field are well represented in the stream function map, Fig. 1a. The poloidal velocity field in the circulation cells alternates its direction from structure to structure. Indications "+" and "−" in the cell centers correspond to positive and negative values of the stream function. The number of these cells located along the radius appears to be nine here and within the whole range of the Rayleigh number 1800≤Ra≤4000. Their horizontal scale, as expected (Chandrasekhar, 1961; Gershuni and Zhukhovitsky, 1972), is comparable with the cylindrical layer height. Cursors in Fig. 1a as well as temperature field isolines in Fig. 1b clearly indicate areas of upward and downward flow. For the obtained state, as is usual with natural convection flows, the azimuthal velocity component is absent, v=0.

Integral characteristic values for this stationary free convection flow are given in Table 1, where U_m, V_m and W_m are used for denoting the maximum absolute values of the radial, azimuthal and vertical velocity component, respectively. Under typical conditions of free convection, horizontal circulation (toroidal field) is not formed because of v=0, and no helicity generation takes place. This results in that V_m, E_k^T and S_Q are found to be equal to zero in this case.

Between a number of natural convection flows, which have been obtained and examined for use as initial distributions, we are choosing one at Ra=3000 to apply the helical forcing and discuss new effects.

6 Structure dynamics, energetics and heat transfer in helical-vortex convection

For the purpose of the current examination some data concerning the linear stability analysis of the plane infinite layer, heated from below and with boundaries that are both rigid, are given for the fundamental mode of instability (n=1) in Fig. 2.

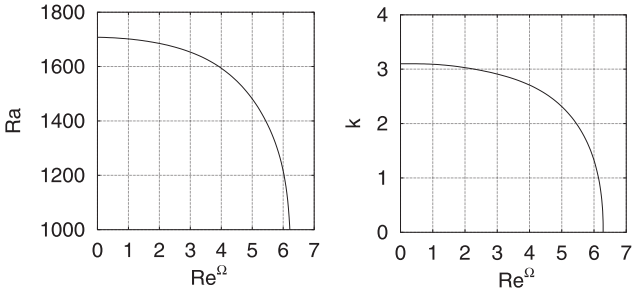

Fig. 2. Minimal critical Rayleigh numbers and corresponding wave numbers versus Re^{Ω} at Pr=1, n=1.

Figure 2 shows the curves $Ra_m(Re^{\Omega})$ and $k_m(Re^{\Omega})$. On both plots one can readily differentiate two regions of quite different response of the examined characteristics: $0<Re^{\Omega}<4$ and $Re^{\Omega}>4$. With a smooth increase in the intensity of helical feedback from 0 to 4, Ra_m and k_m vary rather slowly. Further movement into the region $Re^{\Omega}>4$ causes the dramatic changes in the Ra_m and k_m behavior. Evidently, in this area one may expect the appearance of some new effects and essential rearrangement in the flow pattern.

These data supply us with estimations for the range of parameter Re^{Ω} variation to use in numerical simulation as well as for projected dimensions of arising helical structures.

By varying the Rayleigh and Reynolds numbers widely, $400 \le Ra \le 4000$ and $0 \le Re^{\Omega} \le 6.5$, and using various initial distributions, a few stationary helical-vortex convective states have been obtained.

Applying the helical forcing to the steady-state convection flow assumes the maintenance of the same heating that generates a convective instability and using all the physical fields calculated at Re^{Ω}=0 as initial distributions. Thus, in our simulation the forcing function is not a stirring force but the opposite: helical forcing Eq. (3) is applied to a formed free convection flow and operates further under conditions of existing convective instability. As it is dependent on the velocity field via its spatial derivatives, the forcing is initiated by the same flow that it then affects fairly softly still making the flow helical and supplying it with an additional energy.

Let us examine how the free convection flow is modified under the helical forcing.

6.1 Helicity generation

The analysis of helicity balance equation from Eq. (5) shows that the use of forcing function (3) should result in helicity generation.

The first sign indicating the helical feedback introduced into the convective system is the generation of the toroidal velocity field. Such planar circulation formed by the azimuthal component of velocity is non-typical for natural convection without any complicated factors. Here it is generated from the poloidal field of convective circulation due to the helical feedback.

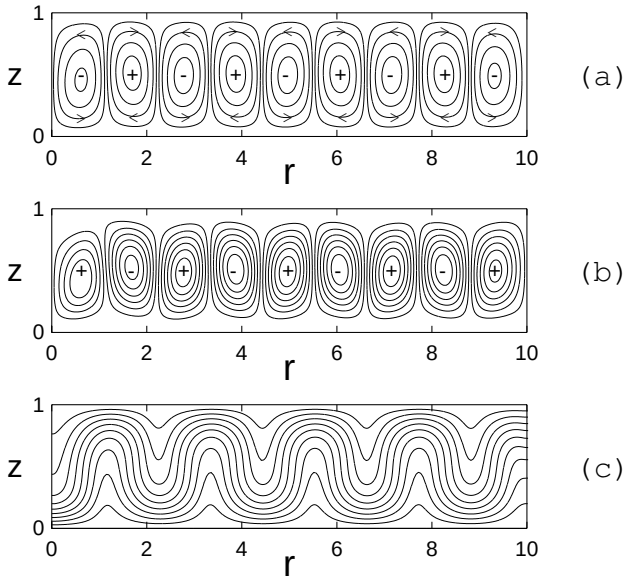

Fig. 3. Isoline maps for the stationary helical convection flow at Re^{Ω}=3, Pr=1 and Ra=3000: **(a)** stream function; **(b)** azimuthal velocity; **(c)** temperature; r=0 corresponds to the axis of symmetry location.

A set of isoline maps including two velocity-related fields and a temperature field at Ra=3000 and Re^{Ω}=3 is presented in Fig. 3.

The isoline map of the azimuthal velocity in the plane (r, z) in Fig. 3b is similar in structure to the corresponding stream function field in Fig. 3a, and the planar circulation also changes its direction from cell to cell. Positive values in Fig. 3b correspond to the counterclockwise circulation seen from the top, whilst the negative azimuthal velocity represents the clockwise circulation in a horizontal plane at z=const. Thus, despite the alternating signs of both poloidal and toroidal circulation from cell to cell, they correlate in that way a superposition of themselves within each convective cell results in the left-handed spiral flow. The examined sample gives us nine left-handed spiral structures within the computational domain. This type of motion should possess some non-zero helicity of the identical sign over the whole flow domain. As a result of the pseudo-scalar nature of this quantity, its sign depends on a frame of reference introduced for the problem under consideration. In the right frame, chosen for the present investigation, the left-handed flow is described by the negative value of helicity. Consequently, the total helicity integrated over the computational domain should be negative as well.

Our numerical problem formulation developed for a confined cylindrical box cannot be valid for any immediate calculation to make a correct and accurate comparison between

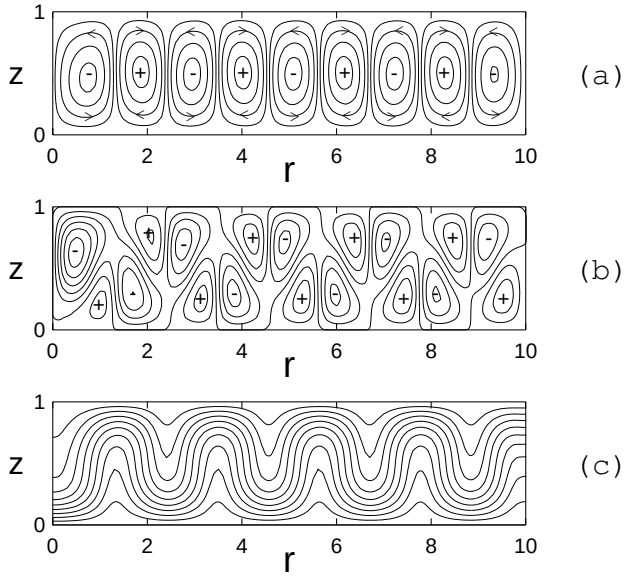

Fig. 4. Isoline maps for the stationary convection flow under the Coriolis force at Re^{Ω}=3, Pr=1 and Ra=3000: **(a)** stream function; **(b)** azimuthal velocity; **(c)** temperature; r=0 corresponds to the axis of symmetry location.

the terms in balance Eqs. (5), which have been derived under assumption of periodic functions and periodic boundary conditions (Frisch, 1995). Nevertheless, we calculated these terms in order to have some qualitative estimations. Indeed, the total helicity of flow found to be negative for all the cases considered in this study. The biggest negative helicity contribution is made by the second term of forcing function, whilst its first term contributes positively. In these conditions the buoyancy force generates negative helicity, and the viscous force participates with positive contribution.

It is appropriate at this stage to compare the effects of applying the helical forcing with the Coriolis force. With this in mind we solved the same equations from system (6) but did so with the Coriolis force introduced into the momentum equation. In this case the dimensionless parameter characterizing the intensity of the Coriolis force was found to be exactly the same, Re^{Ω}, as for the helical forcing. Similar isoline maps at Ra=3000 and Re^{Ω}=3 are shown in Fig. 4.

It may be noted that one velocity-related field in Fig. 4a and the temperature field in Fig. 4c look absolutely identical with the corresponding fields in Fig. 3. However, the azimuthal velocity pattern in Fig. 4b is drastically different from that in Fig. 3b. The azimuthal velocity field generated by the Coriolis force changes its sign along the layer height within each cell of poloidal circulation. The intensity of planar circulation is gradually increased in direction from either boundary where all velocity components vanish. It has a maximum value of a definite sign approximately at half the distance between each boundary and the middle of the layer,

Table 2. Integral characteristic values for the stationary convection flow at Re^{Ω}=3, Pr=1 and Ra=3000: under the Coriolis force (CF) and the helical forcing (HF)

Force	E_k	E_k^T	E_k^P	S_Ω	Nu	U_m	V_m	W_m
CF	244	1	243	22	1.584	11.2	1.1	11.0
HF	299	34	265	−1793	1.621	11.3	6.4	14.8

then, decreasing, reaches zero and changes its sign, and begins increasing again towards the opposite layer boundary. Superposing on poloidal circulation it results in a motion of fluid particles along conical surfaces. Rotation signs are the opposite in the upper and lower cones. This proves to be in good agreement with Chandrasekhar's theoretical results (Chandrasekhar, 1961) and Boubnov and Golitsyn's experiments on rotating convection when they observed cone-like shapes at an initial stage of instability evolution and in the parameter space close to a critical curve (Boubnov and Golitsyn, 1986, 1990). Since the flow helicity in cones from each pair within the same poloidal cell has the opposite signs, the total helicity of the pair may be insignificant. Therefore, for the flow under consideration representing a number of conical pairs, even the appearing flow helicity for a separate pair may be considerably compensated by helicity values in other pairs. As far as we could expect in this case, the flow helicity over the whole computational domain should be close to zero. Indeed, it appears to be insignificant in comparison with the corresponding magnitude for the helical mode given in the lower line in Table 2, and its non-zero value may originate either from the boundary conditions asymmetry or a finite-difference error.

To describe helical convection flow we follow an evolution of the total flow helicity S_Q (Eqs. 8) in addition to other integral characteristics of natural convection. In order to have some more detailed information on the helicity field, it might also be useful to estimate its spatial distribution density. This can be readily accomplished by decomposing the flow area into a few sublayers. In the present study this approach is applied for three horizontal sublayers of equal thickness. In designation the sublayers are counted off from the lower layer boundary (S_{Q1}, S_{Q2}, S_{Q3}), and the absence of the figure in the index denotes a total value of this quantity for the whole flow domain.

Indeed, as far as we could expect from analysis of stream function and azimuthal velocity isoline maps, the flow helicity generated by the helical forcing proves to be negative over the whole computational domain – Fig. 5a. Figure 5b presents another possibility of helicity generation of different signs within the computational domain. This is found to be realized applying the Coriolis force with the same Re^{Ω}=3 to the same initial flow.

The corresponding integral characteristics for both cases can be found in Table 2.

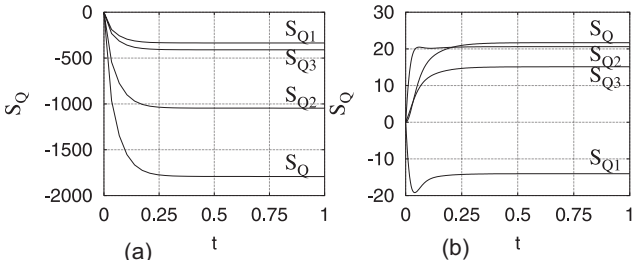

Fig. 5. Helicity evolution at Re^{Ω}=3, Ra=3000 and Pr=1: **(a)** under the helical forcing; **(b)** under the Coriolis force.

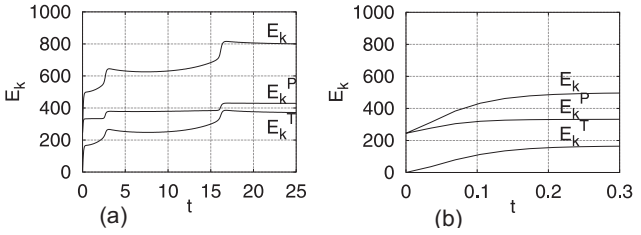

Fig. 6. Flow energetics evolution under the helical forcing at Re^{Ω}=6, Ra=3000 and Pr=1.

Some more interesting results based on these data should be also pointed out. Integral characteristics for the convection generated under the Coriolis force are extremely close to the corresponding values given for the free convection flow in Table 1. Since the Coriolis force does not work, it cannot pump an additional energy into the system. That is why, a toroidal field generation results in a redistribution of the velocity component intensity: an appearance of weak azimuthal velocity leads to a slight decrease of the radial and vertical velocity values. Helical forcing generates a more intensive flow as an examination of all characteristics in Table 2 shows. Though the velocity components, U_m and W_m, forming the poloidal circulation, have fairly close maximum values for both cases, the azimuthal component, V_m, is much greater when generated by the helical forcing. The results also correspond with the values of the kinetic energy – the helical forcing generates a much more intensive toroidal field. The intensity of heat transfer across the layer characterized by the Nusselt number, Nu, is also appreciably higher under the helical forcing. Evidently, to explain these differences in the flow characteristics we have to remember the most essential feature of the helical forcing. Unlike the Coriolis force it creates the positive feedback loop linking the poloidal and toroidal velocity field. To maintain this new feedback the forcing should pump some mechanical energy into the convective system in addition to the heating from below.

As it follows from the kinetic energy balance equation from Eq. (5), this is the case, indeed. However, similarly, to the earlier analysis of helicity balance we can only give some qualitative evaluation based on our rapid calculation. Contributions of buoyancy and viscosity forces are of fixed signs. Evidently, the first of them is positive, and the second is negative. The forcing function contributes in a former manner, i.e. its first and second term generates the energy of opposite sign. However, in this balance equation the first term contributes negatively, and the second does positively. It is very important to note that the positive energy value is several times greater than negative for all examined flows. The positive contribution of forcing increases with increase of the Reynolds number. Thus, for Re^{Ω}=3 the energy pumped by the forcing function into the convective system is found to be five times less than the buoyancy energy. However, at Re^{Ω}=6 quite a different situation takes place: the energy generated by forcing becomes twice as large as the buoyancy energy.

6.2 Positive feedback loop

In order to understand the way the positive helical feedback acts providing a mutual intensification of the velocity components we applied a quantitative analysis of both toroidal and poloidal field evolution using separate variables for the kinetic energy E_k^T and E_k^P, respectively.

Table 3 contains integral characteristics for a number of steady-state helical-vortex convective flows calculated for different Re^{Ω}, and for comparison purposes it begins with the initial distribution data for the free convection flow at Re^{Ω}=0.

As a representative sample that can clearly show the influence of the helical feedback, let us consider, for example, the flow at Re^{Ω}=6. Flow energetics evolution can be traced following Fig. 6 which shows E_k^T and E_k^P as well as total kinetic energy E_k of developing helical convection flow versus time while reaching a steady state.

Kinetic energy values at initial time t=0 are those corresponding to the initial distribution at Ra=3000 and Re^{Ω}=0 which is given in Table 3.

The helical forcing introduced into the system, begins with immediate generation of the toroidal velocity field, and it is this field that appears to be the most responsive to its influence. Figure 6a shows an abrupt increase of the toroidal field energy from E_k^T=0 up to approximately E_k^T=250 within the first two–three time units, and Fig. 6b demonstrates a narrow initial time interval enlarged. The growing toroidal field can be the only reason for changes in the poloidal field intensity. These changes soon become appreciable, although less impressive: the poloidal field is fast growing from E_k^P=245 for initial distribution at t=0 up to $E_k^P \approx$330 within the very first time interval $0<t\leq 0.1$, and later changes more smoothly. As the helical forcing is the only source of mechanical energy in this system, one can consider the increasing poloidal field as a catalyst for further growth in the toroidal field, thereby closing the positive helical feedback loop. Such mutual intensification of velocity components through the feedback loop is observed until the flow reaches a stationary state, as

Table 3. Integral characteristic values for the stationary helical convection flows at Pr=1 and Ra=3000.

Re^{Ω}	E_k	E_k^T	E_k^P	S_{Ω}	Nu	U_m	V_m	W_m
0.0	245	0	245	0	1.586	11.3	0.0	11.1
1.0	251	4	247	-558	1.590	11.3	2.0	11.5
2.0	268	14	254	-1147	1.601	11.4	4.0	12.7
3.0	299	34	265	-1793	1.621	11.3	6.4	14.8
4.0	365	83	282	-2809	1.728	12.7	10.0	10.6
5.0	474	149	325	-4034	1.761	13.1	13.2	14.2
6.0	796	367	429	-7029	1.688	17.0	22.4	13.3
6.3	903	437	466	-8009	1.733	16.4	22.5	15.4
6.5	1422	806	616	-11973	1.959	23.2	37.3	15.7

illustrated by Fig. 6 and Table 3. As one can see by comparing initial (corresponding to Re^{Ω}=0) and final (at Re^{Ω}=6) values of kinetic energy, E_k=245 and E_k=796, this process proves to be very effective: the total kinetic energy E_k of the flow has become more than three times as large.

6.3 Cells merging

Figure 6 demonstrates two well-marked kinks of energy curves corresponding to time values $t\approx$3 and $t\approx$17. Similar qualitative results have been obtained for other flows but only those characterized by Reynolds number $Re^{\Omega}>3.5-4$. To explain this peculiarity we examined the whole set of flow characteristics used in this study as well as referring to the results of linear stability analysis. The theoretical curve in Fig. 2b indicates that one should expect dramatic changes in the typical horizontal scale of structure for Reynolds numbers close to Re^{Ω}=4: this curve shows a considerable broadening of structures. As a result of numerical simulation an enlargement of structure scale by cells merging has been discovered.

It seems to be appropriate to base the search for an explanation of this new phenomenon on other peculiarities of helical convection.

Probably, the most important dynamic feature of convection flow formed under the helical forcing is a generation of the intensive toroidal field. One can find two variables characterizing the toroidal circulation in Table 3: maximum value V_m of the azimuthal velocity and kinetic energy E_k^T. As the corresponding data show this velocity field grows very quickly, far quicker than the poloidal field, with an increase in the Reynolds number. At Reynolds number Re^{Ω}=3 the azimuthal component of velocity V_m=6.4 is still much lower than two other velocity components, U_m=11.3 and W_m=14.8, forming the poloidal field which is usually connected with the thermal convection circulation. At Reynolds number Re^{Ω}=4 the azimuthal velocity V_m=10.0 is found to be extremely close to the maximum value of the vertical velocity W_m=10.6. This means that the azimuthal transfer becomes strong enough to compete against the vertical one. It points out the beginning of a drastic rearrangement in the flow structure and energetics revealing itself at first in the cells merging.

Table 4. Number of cells versus Re^{Ω} in the steady states at Pr=1.

Re^{Ω} =	0	3.5	4	4.5	5	5.5	6	6.5
Ra=2000	9	9	8	8	8	7	6	5
Ra=2500	9	9	8	8	8	7	7	6
Ra=3000	9	9	8	8	8	7	7	6

Table 4 contains calculation results regarding a number of structures within the computational domain for a few values of Rayleigh number. It is evident that instead of nine structures in the initial free convection distribution at Re^{Ω}=0, a resulting helical flow, for example at Re^{Ω}=4, proves to possess eight circulation cells continuously filling up the computational domain. This value of the Reynolds number marks a starting point for the cells merging within a wide range of the Rayleigh number variation up to $Ra\leq$4000 used in our calculations.

The data in Table 4 also illustrate a possibility of a few cells mergers in a developing helical flow. For the flow at Re^{Ω}=6 and Ra=3000 whose energetics evolution is shown in Fig. 6 the number of cells is equal to seven unlike nine cells in the initial distribution. It allows us to interpret two kinks of curves in Fig. 6 as two successive cells merging. In both cases, as the kinetic energy values demonstrate, the cells merging leads to a considerable increase in the flow intensity.

By varying the Reynolds number one can observe up to four merging at Ra=2000 and three merging at Ra=2500 and Ra=3000.

At the Reynolds number Re^{Ω}=4 marking the initiation of cells merging, the total poloidal circulation formed by the vertical and radial velocity components possesses the kinetic energy that is still much greater than the kinetic energy of the toroidal circulation – as Table 3 shows, for Ra=3000 they are E_k^P=282 and E_k^T=83. Table 3 also illustrates the point at which intensities of two velocity fields may become

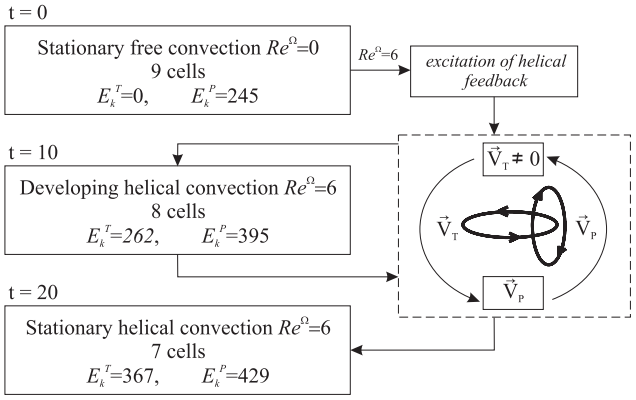

Fig. 7. Scheme of flow intensification through the helical feedback linking the toroidal $\boldsymbol{V}_T$ and poloidal $\boldsymbol{V}_P$ circulation, Ra=3000.

identical at a Reynolds number a little larger than Re^{Ω}=6.3. This value is close to the critical Reynolds number $Re^{\Omega}_{\rm cr}\approx 2\pi$ given by the stability analysis for a fluid layer bounded by two rigid surfaces. As a result, we can propose a quantitative physical interpretation to this special critical value of the Reynolds number: it seems to point out a balance of the poloidal and toroidal velocity field. The larger Reynolds numbers correspond to forced flows under the dominant effect of helical forcing.

6.4 Forced flow

The numerical approach used in the present study allowed us to accurately calculate steady state flows for $0 \leq Re^{\Omega} \leq 6.5$. The obtained results of theoretical and numerical investigation discussed above demonstrate that the range of $0 < Re^{\Omega} < 6.3$ just corresponds to mixed helical-vortex convection flows. In numerical experiments for $Re^{\Omega} > 6.3$ we could observe a few more stationary states until Re^{Ω}=7 which were of forced origin. For $Re^{\Omega} > 6.6$ the flow intensity increases sharply, and in the flow domain there appear clearly pronounced velocity and temperature boundary layers. Studies of these phenomena require the higher spatial resolution, and different numerical and computing techniques.

However, at this point it is worth discussing an example of pronounced forced flow to present the peculiarities of the developing helical-vortex instability and compare it with the mixed flow in which the effects of both helical-vortex and convective instability are strong. To this end let us choose flows characterized by the Reynolds number Re^{Ω}=6.4. In this case at Ra=3000 we still have a good sample of the convection effects. On the other hand, it is already, at this point, in no need of any heating (i.e. Ra=0) to generate an intensive stationary vortex flow, whilst slightly lower Reynolds numbers $Re^{\Omega} < 6.4$ did not give any instability in isothermal conditions. In addition to the two afore-mentioned flows it seemed useful to examine an intermediate example. We chose a flow at Ra=1100. This value is slightly higher than the Rayleigh number $Ra_3^* \approx 1071$ given by the stability analysis in Appendix B for the wave number tending to zero at $Re^{\Omega}_{\rm cr} \approx 2\pi$. Characteristics of the chosen flows are given in Table 5, where n denotes the number of cells.

Qualitative data from Table 5 as well as a number of others which were presented early are interpreted and summarized in the next section.

6.5 Peculiarities of energetics and heat transfer

The new effects found in the flow structure and dynamics can be explained on the basis of flow energetics.

In free convection flow without any complicated effects there is a single energy source which is the layer heating. The existence of a stationary convective regime, for example as it is for Ra=3000 and Re^{Ω}=0 in our study, corresponds to the energy balance: the energy supplied into the system by the layer heating from below is transformed into the kinetic energy of convective motions, and the remaining part dissipates due to viscosity and boundary friction.

The situation is changed when the helical forcing is introduced into the convective system. This initiates an additional energy source simulating an energy flux from the small-scale helical turbulence. Certainly, its energy also scatters a little but the greater part is contributed to the kinetic flow energy. This contribution is effectively made through a positive feedback loop and results in a very impressive flow intensification. This is well illustrated by the quantitative data in Table 3 and Fig. 6 as well as by Fig. 7 presenting a scheme of helical convective flow intensification:

An intrinsic feature of helical-vortex convective flow is a powerful toroidal circulation. Immediately the helical forcing intensity reaches some critical level at the Reynolds number $Re^{\Omega} \approx 4$, this velocity field begins to contribute significantly to the flow structure and energetics by merging convective cells and thereby breaking down the typical convective circulation. This process results not only in the increase of kinetic energy but also in the marked intensification of the heat transfer. When analyzing data from both Table 3 and Table 4 one can first find a very smooth growing of heat flux, Nu. It concerns the nine-cells flow structure existing within $0 < Re^{\Omega} < 4$. A transition to the eight-cells pattern at $Re^{\Omega} \approx 4$ is accompanied by a marked increase in the Nusselt number. This can only mean that a new flow pattern proves to be the more optimal means of heat transfer. Data in Table 4 also show that the intensification of convection impedes the cells merging: the flow pattern for Re^{Ω}=6.5 consists of five helical vortex convective cells at Ra=2000 whilst at higher Rayleigh numbers, Ra=2500 and Ra=3000, one can observe the six-cells flow structure.

Let us now refer to Table 5 containing data for three stationary flows generated under the dominant effect of helical forcing at the same Reynolds number Re^{Ω}=6.4. This implies the identical power of the helical energy source. Thus,

Table 5. Integral characteristic values versus Ra for the stationary helical flows at Re^{Ω}=6.4 and $Pr = 1$.

Ra	E_k	E_k^T	E_k^P	S_Ω	Nu	U_m	V_m	W_m	n
0	1007	751	256	−6440	0	14.9	29.2	3.6	1
1100	4335	3229	1106	−27981	1.646	30.6	58.6	11.1	1
3000	1380	785	595	−11525	1.729	22.6	37.1	15.1	6

we can compare the efficiency of energetics processes in three different cases.

In the first case the helical forcing as a single energy source generates an intensive isothermal helical-vortex flow. In this state the energy of poloidal circulation E_k^P=256 is three times as weak as that of E_k^T=751 of the toroidal field. In the second and the third example the flows result from a combined situation of two energy sources: heating from below and helical forcing.

Without doubt, the second regime demonstrates the highest efficiency in that it concerns the helical source energy transformation into the kinetic energy of vortex flow. When giving an explanation of this phenomenon, the particular emphasis should be placed on the cell number n in the compared flows. In the first and the second example the flow pattern consists of a single large vortex cell occupying the whole computational domain whilst in the third case one can observe the six-cells flow structure. The total kinetic energy at Ra=1100 is much larger than that for Ra=3000. Evidently, in the system with helical-vortex instability, the flow structure in the form of a single large-scale helical vortex is optimal from the energetics point of view. From the very beginning this instability evolution is accompanied by the development of the azimuthal flow. This flow generates the cells merging which suppresses free convection heat transfer through the layer. Typical natural convection flow structure realized as a multitude of small circulation cells with up- and downward flows is changed by a single helical vortex cell. As a result, it decreases energy losses due to dissipation. The latter is well illustrated by comparing the second and third flow characteristics. It is only worth comparing their total kinetic energy values, E_k=4335 and E_k=1380, bearing in mind that the second energy value corresponds to much more intensive heating from below.

Introduction of the helical forcing into the system qualitatively changes the heat transfer. Free convection heat transfer realized at Re^{Ω}=0 by the poloidal circulation is replaced by the mixed convection with pronounced azimuthal circulation. Thus, the helical forcing effect results in the more complicated trajectories of fluid particles compared with the natural convective flow: both rising of the warm and lowering of the cold fluid within every vortex cell follow helical paths.

Comparing free convection heat flux Nu=1.586 at Ra=3000 (nine-cells flow pattern) with data within the six-cells helical flow structure at the same Ra=3000 one can find the more intensive heat transfer Nu=1.729 (Table 5). Moreover, even at the far lower Rayleigh number of Ra=1100 (single helical vortex) the heat flux, Nu=1.646, exceeds its free convection value. Therefore, we can conclude that the observed rearrangement in the flow structure and dynamics intensifies the heat transfer through the layer.

7 Conclusion

Our two-stages strategy for numerical simulation of helical-vortex effects in Rayleigh-Bénard convection with a large aspect ratio includes:

- forcing simulation of helical-vortex laminar and turbulent convection by introducing the model force into the Boussinesq equations;
- direct numerical simulation (DNS) of developed turbulent convection in a rotating fluid with internal heat sources.

The main idea of the search strategy is the application of a forcing function which can have a physical interpretation. As a result of averaging under developing the mean-field equation for the hydrodynamic alpha-effect, this function parameterizes the influence of small-scale helical turbulence generated in a rotating fluid with internal heat sources.

It is worth particular note that persistent efforts were necessary to achieve this result in helical term of this kind in the mean-field velocity equation. Constant temperature difference or constant heat flux could not produce a sufficient temperature inhomogeneity. Additional heat generation by internal sources throughout the rotating fluid layer proved to be a necessary condition to initiate the helical-vortex instability. This may well explain why no sign of large-scale helical-vortex instability has been discovered in numerous studies on rotating turbulent convection which were without internal heat release. Comparing the effects of the Coriolis force and the helical forcing carried out by numerical simulation in the present investigation also gives convincing arguments that support this view.

Unlike the Coriolis force, the helical forcing can initiate a positive feedback between the poloidal and toroidal components of the vector velocity field and maintain it by ensuring an additional energy influx. This feedback is responsible for the generation of large-scale helical-vortex instability resulting in the new effects shown and discussed in this paper.

The results of the first step in modeling are presented in this study. The application of the forcing initially to a numerical simulation of laminar helical convection allowed us to obtain new effects in the flow structure and energetics, which might be of immediate relevance to the initiation of large-scale instability in turbulent states. The most important finding is an enlargement of the typical horizontal scale of the forming helical convective structures accompanied by a cells merging, an essential increase in the kinetic energy of flows and intensification of heat transfer. The results of modeling allow explaining how the helical feedback can work providing the non-zero mean helicity generation and the mutual intensification of poloidal and toroidal circulation, and demonstrate how the energy of the additional helical source can be effectively converted into the energy of intensive large-scale vortex flow. Direct numerical simulation has started with using the helical forcing (Burylov et al., 2004).

It seems interesting to try the inclusion of the proposed helical forcing in mathematical models describing the development of tropical depressions to evaluate the possible effect of helical feedback linking the horizontal and vertical circulation and compare it with contributions of significant mechanisms involved in this early stage of the cyclogenesis. Another important application may be found in investigations of magneto-convection processes in atmospheres of Sun and stars.

Appendix A

The mean-field equation for the turbulent vortex dynamo in a convectively unstable rotating fluid

The first example of large-scale alpha-like instability in hydrodynamics of non-conducting fluid was discovered by Moiseev et al. (1983b) for homogeneous isotropic helical turbulence in a compressible medium. Moreover, further investigations have demonstrated that this example is the simplest in the sense of mathematical description. Indeed, helicity of the velocity field is mathematically represented by nonzero pseudoscalar $\alpha \sim \langle <\boldsymbol{v}\cdot\mathrm{curl}\boldsymbol{v}\rangle > \neq 0$. For a compressible fluid due to asymmetry of the Reynolds stress tensor this has found to be sufficient to obtain after averaging the generating alpha-term, $\mathrm{curl}(\alpha\boldsymbol{\omega})$, describing the mean vorticity of the large-scale flow. It is precisely this term that allows us to obtain the solution ensuring an exponential growth of vorticity.

For an incompressible medium the situation is quite different. If the turbulence is homogeneous and isotropic, the break of reflection symmetry generating nonzero helicity of the small-scale velocity field is not a sufficient condition for the existence of $H\alpha$-effect. This is attributed to the fact that in incompressible flows the Reynolds stress tensor is symmetrical. Therefore, when developing an equation for mean vorticity of the velocity field the pseudoscalar coefficient α must necessarily vanish. This implies that some additional factors are needed for the symmetry break enabling us to construct a generating term in the averaged equations.

The first example of a vortex dynamo for homogeneous isotropic helical turbulence in an incompressible fluid was discovered by Moiseev et al. (1988). In this case, the additional factors breaking the symmetry were the gravity force and the temperature gradient. A mathematical description of $H\alpha$-effect developed in this work is more sophisticated than for a compressible medium. In their mathematical model of the $H\alpha$-effect Moiseev et al. (1988) postulated the helical turbulence existence directly at the very initial step of the problem formulation. This suggests that such a break of reflection invariance of small-scale turbulence can be produced by a combined action of vertical inhomogeneity (for example, by stratification sufficiently unstable for convection initiation) and the Coriolis force.

An attempt to incorporate these factors explicitly into the mean-field model by parameterizing the process of helicity generation on small scales was made by Rutkevich (1993). To this end, turbulent convection was considered in a rotating horizontal layer of incompressible liquid. Rutkevich (1993) did not postulate turbulence helicity in the initial problem formulation. Small-scale turbulence was modeled as that driven by a random external force and considered as highly anisotropic. The inverse influence of small-scale convection on the temperature gradient was taken into account what resulted in a large-scale temperature profile which was closer to a neutral one.

Assuming that the linear temperature gradient generated by uniform temperature difference between the layer boundaries is unable to ensure vertical inhomogeneity necessary for initiating a large-scale instability, Rutkevich (1993) suggested the inclusion of additional inhomogeneity in the problem formulation. Volumetric heating of the layer by internal sources was taken into account providing a temperature profile in the form of square parabola. Convective flow was considered in a layer of thickness λ bounded above and below by a fluid with slightly stable stratification. Unstable stratification within the layer was provided by both heating from below and uniformly distributed internal heat sources. Temperature profile was specified as a Taylor expansion along the vertical direction z, and its curvature assumed to be insignificant:

$$T_0(z) = \mathrm{const} - Az - \frac{B}{2}z^2 + \ldots, \qquad \text{(A1)}$$

$$A, B > 0, \qquad A \gg \frac{B}{2}\lambda.$$

Convection of this kind was considered by Gribov and Gurevich (1956) and by Julien et al. (1996) for a rotating layer. The convection threshold for these conditions was found to be lower than for a layer bounded from above and below, and convective flows were found to be elongated along the vertical direction due to the effect of penetrative convection.

The efforts made in this direction led to the following mean-field equation (Rutkevich, 1993):

$$\left(\frac{\partial}{\partial t} - \Delta\right)\langle v_i\rangle + Ta^{1/2}\, P_{im}\varepsilon_{msj} e_s \langle v_j\rangle = \\ = s_1 P_{im}\nabla_k \left(e_m\varepsilon_{kra} + e_k\varepsilon_{mra}\right) e_r \langle v_a\rangle \quad \text{(A2)}$$

Here, $\langle v_i\rangle$ is the mean velocity field, P_{im} is a projection operator eliminating a potential part of the velocity field, e_i the unit vector directed vertically upward, ε_{ijk} the antisymmetrical Levi-Chivita tensor. As investigations on helical turbulence in magnetohydrodynamics (Krause and Rädler, 1980) have shown, the terms with tensor ε_{ijk} are responsible for initiating large-scale instability. By analogy with the hydromagnetic equation for alpha-effect, the expression on the right of Eq. (A2) involving helicity of the velocity field can be named the alpha-term. Equation (A2) differs from the early model (Eq. 1) by the Taylor number Ta term characterizing the fluid layer rotation. Another difference is an absence of the Rayleigh number term describing convection on large scales that is a result of taking into account the influence of small-scale convection on the temperature gradient over the whole layer height. The expression on the right of Eq. (A2) involves the Reynolds stresses with helical terms. This indicates that under examined conditions a homogeneous small-scale anisotropic turbulence becomes helical.

The governing parameters in Eq. (A2) are the Taylor number $Ta^{1/2}=2\Omega h^2/\nu_T$ and the coefficient s_1 in front of the alpha-term. This coefficient depends on physical parameters of fluid and turbulence characteristics in a rather complicated manner (Rutkevich, 1993):

$$s_1 = 2\Omega\tau\eta^2 \frac{E\tau^2}{\lambda^2}\frac{h}{\lambda}\frac{\nu}{\nu_T}\frac{B\lambda}{A}, \quad \text{(A3)}$$

where Ω is the angular velocity of fluid layer rotation, E is the density of turbulence energy, λ and τ are the most energetic scale and characteristic time of the turbulent velocity correlation, A is the constant temperature gradient between the horizontal boundaries of the layer, B is a coefficient characterizing the power of internal heat sources, h is the layer height, ν is the molecular coefficient of kinematic viscosity, ν_T is the coefficient of turbulent viscosity on the large scale, η is a dimensionless parameter specifying the aspect ratio (of typical vertical to horizontal dimension) for small-scale convective structures.

It should be noted that here the coefficient before the alpha-term does not contain the prescribed helicity of small-scale turbulence. Now the parameter s_1 is found to be dependent on the density of turbulence energy, the Coriolis force and the measure of nonlinearity of the temperature gradient.

The most important achievement reached as a result of analysis of Eq. (A2) and having considerable significance in the development of the hydrodynamic alpha-effect theory is that which concerns the effect of internal heat release. Parameter s_1 includes a ratio B/A formed by coefficients describing the temperature profile in expression (A1) for initial problem formulation (Rutkevich, 1993). In the absence of internal heat release ($B=0$) the excitation of large-scale instability is impossible since heating from below ($A\neq 0$) is not a sufficient condition for generating the vortex dynamo effect.

Therefore, following Rutkevich (1993), we may conclude that in the case of convectively unstable fluid the concept of turbulence helicity suggests a parameterization of the combined effect of the Coriolis force and internal heat release. The obtained result provides every reason to consider the process of free convection under the above conditions as an effective mechanism for turbulence helicity generation on small scales.

Appendix B

Linear stability analysis: plane horizontal layer

Let us consider a horizontal fluid layer $0<z<h$ bounded below and above by two parallel planes and infinite in the x and y directions. Its lower and upper boundaries are maintained at constant and different temperatures, T_1 and T_2, respectively, so that the positive Rayleigh number $Ra>0$ corresponds to the heating from below whilst $Ra<0$ is for the above heated layer. The hydrodynamic boundary conditions include three cases: both lower and upper surfaces are free or rigid, and the mixed situation consisting of their combination.

In the limiting case $Re^{\Omega}=0$ system (Eq. 6) is reduced to the Boussinesq equations whose solutions for different boundary conditions were carefully analyzed in Chandrasekhar (1961); Gershuni and Zhukhovitsky (1972) by both the methods of linear and nonlinear theory of hydrodynamic stability. The convective instability only arises after exceeding some critical Rayleigh number and evolves into a flow pattern consisting of numerous small cells. The cells are created by poloidal circulation, each having the characteristic horizontal dimension of the order of layer height. This corresponds to the well-known Rayleigh-Bénard convection (Chandrasekhar, 1961; Gershuni and Zhukhovitsky, 1972).

Equations (6) at $Ra\neq 0$ and $Re^{\Omega}\neq 0$ have the steady solution corresponding to a mechanical equilibrium which we consider as a basic state.

We examine the conditions under which the quiescent solution is unstable against small non-stationary disturbances depending exponentially on time and periodic in the x and y directions.

Thermal and hydrodynamic boundary conditions for the disturbance amplitudes in the case of both isothermal bounding surfaces can be written in dimensionless form as

$$T = 0, \quad \text{at} \quad z = 0;\ 1,$$
$$\text{rigid boundary}: \quad \boldsymbol{V} = 0, \quad \text{(B1)}$$

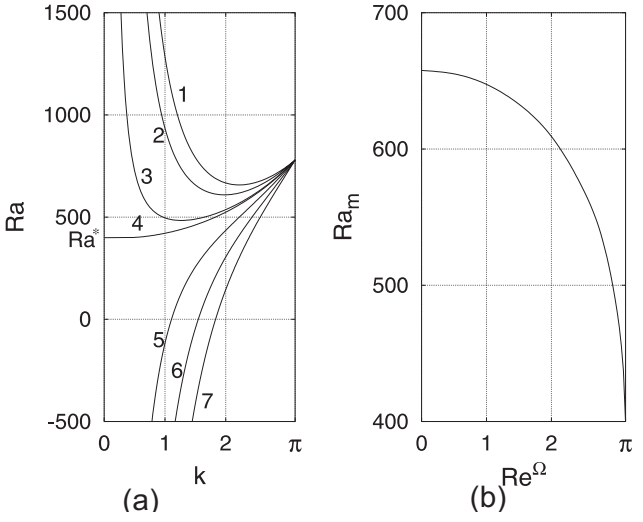

Fig. B1. (a) Neutral curves $Ra(k)$ for Re^{Ω} (1) 0.0; (2) 2.0; (3) 3.0; (4) π; (5) 4.0; (6) 5.0; (7) 6.0; and **(b)** minimal critical Rayleigh number versus helical feedback intensity Re^{Ω} at Pr=1, n=1.

$$\text{free boundary}: \quad w = 0, \quad \frac{\partial u}{\partial z} = \frac{\partial v}{\partial z} = 0.$$

The analysis of stability has been accomplished following the standard procedure discussed in detail in Chandrasekhar (1961); Gershuni and Zhukhovitsky (1972). For the problem under consideration describing the helical convection, the spectrum of disturbances is found to be dependent on three parameters: Ra, Pr and Re^{Ω}.

In the general case the spectral problem for the disturbance amplitudes can be solved numerically, for example, by the Runge-Kutta method with an automatic step selection.

Specifying Pr=1 we could considerably simplify the spectral problem formulation and analytically obtain its exact solution in the case of the fluid layer bounded by two free surfaces.

B1 Instability of fluid layer with free boundaries

In the case Re^{Ω}=0, we obtain the classical Rayleigh problem which has an analytical solution given, for example, in monograph (Gershuni and Zhukhovitsky, 1972): the minimal (i.e. lowest from the possible ones for disturbances of different scale) critical Rayleigh number marking the onset of convection is Ra_m=657.511, and the corresponding wave number is k_m=2.221. Our numerical method applied to this problem yields the highly close values Ra_m=657.512 and k_m=2.221.

To trace the effect of the helical feedback introduced into the system at $Re^{\Omega}\neq 0$, the following formula was obtained for the neutral curve:

$$Ra = \frac{(n^2\pi^2 + k^2)^3 - (Re^{\Omega})^2 n^2\pi^2(n^2\pi^2 - k^2)}{k^2} \qquad \text{(B2)}$$

which decides the critical Rayleigh number marking the instability onset against the disturbance with the prescribed k and n. Here, k and n define the horizontal and vertical scale of the disturbance, respectively. The lowest critical Rayleigh number can be found for a fundamental mode of instability characterized by n=1. By changing Re^{Ω} one can obtain the neutral curves located in the plane (Ra, k).

Figure B1 demonstrates the neutral stability curves at n=1 for a number of parameter Re^{Ω}, including Re^{Ω}=0 – left panel, whilst in the right panel the minimal critical Rayleigh number Ra_m versus Re^{Ω} is presented.

The minimum of neutral curve 1 for Re^{Ω}=0, marking the natural convection onset at some threshold value $Ra_m\approx$658, is located within a medium wave number area at $k_m\approx$2.2 – Fig. 7a.

The effect of the helical feedback generation ($Re^{\Omega}\neq 0$) results in reduction of the threshold of convective instability: the critical Rayleigh number decreases with the increase of the parameter Re^{Ω} – Fig. 7b. It means that this new factor appeared in the system, in addition to the buoyancy affects a warmer and lighter fluid causing it to rise from the heated lower boundary.

The minimum of neutral stability curves is shifted to small wave numbers (long wave domain), implying the growth of typical horizontal scale of arising structures. With the parameter Re^{Ω} approaching some critical value $Re^{\Omega}_{\rm cr}=\pi$, the threshold Rayleigh number tends to a limit value $Ra^*=4\pi^4\approx$390 whilst the wave number tends to zero. Formally, this corresponds to an infinite horizontal dimension of a supercritical flow and suggests profound changes in the flow pattern compared with the natural convection: instead of a set of relatively small cells there appears a large scale structure that occupies the whole available space.

The curve $Ra(k)$ at $Re^{\Omega}_{\rm cr}=\pi$ also serves as a boundary separating two domains within which the solutions display a quite different behavior. Above it the neutral curves have minima, the stability domain is contiguous to the vertical Ra-axis and contains the solutions with comparably smaller wave numbers, i.e. corresponding to the longer waves. Below the separating curve $Re^{\Omega}_{\rm cr}=\pi$ the picture is just opposite: the unstable solutions area adjoins the Ra-axis whilst the domain of stability is located to the right from the neutral curves and towards the larger wave numbers (shorter waves). The lower neutral curves have no minima and carry on over a domain of negative Rayleigh numbers.

The helical forcing can generate a vortex flow for $Re^{\Omega} > Re^{\Omega}_{\rm cr}=\pi$ in the absence of any temperature inhomogeneity (Ra=0).

Moreover, if $Re^{\Omega} > Re^{\Omega}_{\rm cr}=\pi$ some instability can be generated for any Rayleigh number, and even in conditions of heating from above that is usually impossible in natural convection flows without any complicated factors. This demonstrates the dominant effect of helical forcing for $Re^{\Omega} > \pi$ and corresponds to forced convection flows.

Thus, important conclusions following from the above consideration are worth to note particularly: the helical forcing operates favoring the long wave flow generation and decreasing the threshold of instability.

B2 Instability of fluid layers with rigid and mixed boundaries

In this formulation the full analysis of the corresponding stability problem even for the natural convection flow at Re^{Ω}=0 could be carried out only by using some numerical methods (Gershuni and Zhukhovitsky, 1972).

To investigate the conditions of the onset of helical convection flow we applied the same numerical approach used and tested for the layer with free boundaries. It resulted in data that follow.

For the onset of natural convection flow at Re^{Ω}=0, we obtained for the fundamental mode of instability ($n = 1$) that the critical Rayleigh number with the corresponding wave number were $Ra_m \approx 1707.967$ and $k_m \approx 3.117$ (rigid boundaries); $Ra_m \approx 1100.777$ and $k_m \approx 2.682$ (mixed boundaries). They are found to be in a very good agreement with the similar values from Gershuni and Zhukhovitsky (1972): $Ra_m \approx 1707.762$ and $k_m \approx 3.116$; $Ra_m \approx 1100.657$ and $k_m \approx 2.682$ for rigid and mixed boundaries, respectively.

For all three types of boundary conditions the neutral curves display the similar behavior only differing in the instability threshold values as well as in the limit Reynolds numbers which correspond to a border (Ra, k) separating the regions of different neutral curve behavior in the plane (Ra, k). The borders are found to be located at $Re^{\Omega}_{\rm cr} \approx 1.5\pi$ for the mixed boundaries and at $Re^{\Omega}_{\rm cr} \approx 2\pi$ for the rigid ones.

According to expectations, the threshold Rayleigh number at any fixed Reynolds number proves to be the highest for the fluid layer with both rigid boundaries. The approximate limit Rayleigh numbers corresponding to the wave number tending to zero have been also found (n=1) : $Ra^*_1 \approx 390$ is for the layer with free boundaries, $Ra^*_2 \approx 682$ – with the mixed and $Ra^*_3 \approx 1071$ – with the rigid.

Acknowledgements. We would like to thank P. G. Frick for his constant support, M. V. Kurgansky for reading and discussing our manuscript, P. B. Rutkevich and R. A. Stepanov for important remarks. We thank A. Brandenburg for the discussion concerning an appropriate helical forcing what provoked our two stages strategy substantiated in this paper, L. Kh. Ingel and A. P. Khain for drawing our attention to a possible application of our forcing in numerical models for tropical cyclone. Our special thanks to F. Labram from Southampton who worked on our manuscript for the "Advances in Fluid Mechanics" as an editor at WIT Press five years ago and has been so kind as to help us again with the editorial revision of the manuscript. This work is supported by the Russian Foundation for Basic Research under Grants No. 04-05-64315, 03-05-64593 and the International Science and Technology Center under Project No. 2021.

Edited by: N. S. Erokhin
Reviewed by: three referees

References

Berezin, Y. and Zhukov, V.: Convective instability in a medium with helical turbulence, Z. Prikl. Mekh. Techn. Fiz. (in Russian), 1, 61–66, 1990.

Bogatyryov, G.: Excitation of cyclonic vortex or a laboratory model of tropical cyclone, JETP Lett., 51, 630–633, 1990.

Bogatyryov, G. and Smorodin, B.: Physical model of the rotation of a tropical cyclone, JETP Lett, 63, 28–32, 1996.

Bogatyryov, G., Kolesnichenko, I., Levina, G., and Sukhanovsky, A.: Laboratory model for process of large-scale spiral vortex formation in a convectively unstable rotating fluid, Izv. Russ. Acad. Sci., Atmos. Oceanic Phys., 42(4), 1–7, 2006.

Boubnov, B. and Golitsyn, G.: Experimental study of convective structures in rotating fluids, J. Fluid Mech., 167, 503–531, 1986.

Boubnov, B. and Golitsyn, G.: Temperature and velocity field regimes of convective motions in a rotating plane fluid layer, J. Fluid Mech., 219, 215–239, 1990.

Brandenburg, A. and v. Rekowski, B.: Astrophysical significance of the anisotropic kinetic alpha effect, Astron. Astrophys., 379, 1153–1159, 2001.

Burylov, I., Firulyov, A., and Levina, G.: Numerical modeling of helical-vortex convective flows, Advances in Turbulence X., edited by: Andersson, H. I. and Krogstad, P.-A., p. 201–204, 2004.

Busse, F.: Transition to turbulence in Rayleigh-Benard convection, Series: Topics in Applied Physics. Hydrodynamic Instabilities and the Transition to Turbulence, edited by: Swinney, H. L. and Gollub, J. P., 45, 111–162, 1981.

Chandrasekhar, S.: Hydrodynamic and Hydromagnetic Stability, Dover, New York, 1961.

Frisch, U.: Turbulence, Cambridge University Press, Cambridge, 1995.

Frisch, U., She, Z., and Sulem, P.: Large-scale flow driven by the anisotropic kinetic alpha effect, Physica, 28D, 382–392, 1987.

Gershuni, G. and Zhukhovitsky, E.: Convective Stability of Incompressible Fluid (Engl. transl: Keterpress, Jerusalem, 1976), Nauka, Moscow, 1972.

Golitsyn, G.: Simple theoretical and experimental study of convection with some geophysical applications and analogies, J. Fluid Mech., 95, 567–608, 1979.

Gribov, V. and Gurevich, L.: To stability theory of the layer under overadiabatic temperature gradient in the gravity field, Zh. Eksp. Teor. Fiz. (in Russian), 5, 854–864, 1956.

Julien, K., Legg, S., McWilliams, J., and Werne, J.: Penetrative convection in rapidly rotating flows: preliminary results from numerical simiulation, Dyn. Atmos. Oceans, 24, 237–249, 1996.

Kitchatinov, L., Rüdiger, G., and Khomenko, G.: Large-scale vortices in rotating stratified disks, Astron. Astrophys., 287, 320–324, 1994.

Kolesnichenko, I., Levina, G., and Sukhanovsky, A.: Experimental attempt for controlling the large-scale rotating spiral vortex, Advances in Turbulence IX., edited by: Castro, I. P., Hancock, P. E., and Thomas, T. G., p. 173–176, 2002.

Krause, F. and Rädler, K.-H.: Mean-Field Magnetohydrodynamics and Dynamo Theory, Academie-Verlag, Berlin, 1980.

Kurgansky, M.: Generation of helicity in a moist atmosphere, Izv. Russ. Acad. Sci, Atmos. Oceanic Phys., 29(4), 444–448, 1993.

Kurgansky, M.: Vorticity generation in a moist atmosphere, Izv. Russ. Acad. Sci., Atmos. Oceanic Phys., 34(2), 156–161, 1998.

Kurgansky, M.: Vorticity genesis in the moist atmosphere, Phys. Chem. Earth (B), 24, 959–961, 1999.

Kurgansky, M.: Adiabatic Invariants in Large-Scale Atmospheric Dynamics, Taylor & Francis, London and New York, 2002.

Levina, G., Moiseev, S., and Rutkevich, P.: Hydrodynamic alpha-effect in a convective system., Chapter 4, in: Nonlinear Instability, Chaos and Turbulence, Vol. 2, edited by: Debnath, L. and Riahi, D. N., Advances in Fluid Mechanics Series, 25, 111–162, 2000.

Levina, G., Firulyov, A., and Shestakova, L.: Numerical simulation of evolution of helical-vortex instability in a fluid layer heated from below, Izv. Russ. Acad. Sci., Fluid Dyn., 36(4), 538–547, 2001.

Levina, G., Burylov, I., Firulyov, A., and Shestakova, L.: Helical-vortex instability in a convectively unstable fluid: origin and numerical simulation, Preprint ICMM UB RAS, 1–60, 2004.

Lyubimov, D. and Smorodin, B.: On convective instability of plane horizontal layer with helical turbulent fluid, Preprint IMSS (in Russian), p. 3–45, 1989.

Moffatt, H.: Magnetic Field Generation in Electrically Conducting Fluids, Cambridge University Press, Cambridge, 1978.

Moiseev, S., Sagdeev, R., Tur, A., Khomenko, G., and Shukurov, A.: Physical mechanism of amplification of vortex disturbances in the atmosphere, Sov. Phys. Dokl., 28, 925–928, 1983a.

Moiseev, S., Sagdeev, R., Tur, A., Khomenko, G., and Yanovsky, V.: A theory of large-scale structure origination in hydrodynamic turbulence, Sov. Phys. JETP, 58, 1149–1157, 1983b.

Moiseev, S., Rutkevich, P., Tur, A., and Yanovsky, V.: Vortex dynamos in a helical turbulent convection, Sov. Phys. JETP, 67, 294–299, 1988.

Parker, E.: Cosmical Magnetic Fields, Clarendon Press, Oxford, 1979.

Pipin, V., Rüdiger, G., and Kitchatinov, L.: The rotational quenching of the rotation-induced kinetic alpha-effect, Geophys. Astrophys. Fluid Dyn., 83, 119–133, 1996.

Rutkevich, P.: Equation for vortex instability caused by convective turbulence and the Coriolis force, JETP, 77, 933–938, 1993.

Steenbeck, M., Krause, F., and Rädler, K.-H.: Zur Berechnung der mittleren Lorentz-Feldstärke $\overline{\mathbf{v}\times\mathbf{B}}$ für ein elektrisch leitendes Medium in turbulenter, durch Coriolis-Kräfte beeinflusster Bewegung, Z. Naturforsch, 21a, 369–376, 1966.